

Article

# Diel Variability of $p\text{CO}_2$ and $\text{CO}_2$ Outgassing from the Lower Mississippi River: Implications for Riverine $\text{CO}_2$ Outgassing Estimation

Jeremy H. Reiman<sup>1</sup> and Y. Jun Xu<sup>1,2,\*</sup> 

<sup>1</sup> School of Renewable Natural Resources, Louisiana State University Agricultural Center, Baton Rouge, LA 70803, USA; jreima1@lsu.edu

<sup>2</sup> Coastal Studies Institute, Louisiana State University, Baton Rouge, LA 70803, USA

\* Correspondence: yjxu@lsu.edu; Tel.: +1-225-578-4168

Received: 19 October 2018; Accepted: 21 December 2018; Published: 27 December 2018



**Abstract:** Carbon dioxide ( $\text{CO}_2$ ) outgassing from river surface waters is an important component of the global carbon cycle currently not well constrained. To test the hypothesis that riverine partial pressure of  $\text{CO}_2$  ( $p\text{CO}_2$ ) and  $\text{CO}_2$  outgassing rates differ between daylight and darkness, we conducted in-situ  $p\text{CO}_2$  and ambient water measurements over four 24-h periods in the spring and summer of 2018 in the Lower Mississippi River under varying flow regimes. We hypothesized that diel  $p\text{CO}_2$  variation will correlate inversely with solar radiation due to light-induced photosynthesis. Despite differing ambient conditions between seasons, we found a consistent diel cycle of riverine  $p\text{CO}_2$ , with highest values before sunset and lowest values during peak daylight. Recorded  $p\text{CO}_2$  measurements varied by 206–607  $\mu\text{atm}$  in spring and 344–377  $\mu\text{atm}$  in summer, with significantly lower records during daylight in summer.  $\text{CO}_2$  outgassing was significantly lower during daylight in both seasons, with diel variation ranging between 1.5–4.4  $\text{mmol m}^{-2} \text{h}^{-1}$  in spring and 1.9–2.1  $\text{mmol m}^{-2} \text{h}^{-1}$  in summer. Daily outgassing rates calculated incorporating diel variation resulted in significantly greater rates ( $26.2 \pm \text{std. } 12.7 \text{ mmol m}^{-2} \text{d}^{-1}$ ) than calculations using a single daily  $p\text{CO}_2$  value. This study suggests a likely substantial underestimation of carbon outgassed from higher order rivers that make up a majority of the global river water surface. The findings highlight the need for high temporal resolution data and further research on diel  $\text{CO}_2$  outgassing in different climate regions to constrain uncertainties in riverine flux estimation.

**Keywords:** aquatic carbon cycle; freshwater  $\text{CO}_2$ ; diel river metabolism; river carbon accounting; Mississippi River

## 1. Introduction

Outgassing of carbon dioxide ( $\text{CO}_2$ ) from rivers has been identified as a significant piece of the carbon cycle [1–3]. The process has been attributed to an oversaturation of dissolved  $\text{CO}_2$  in the water column, resulting in diffusion of  $\text{CO}_2$  into the atmosphere. The two primary inputs of  $\text{CO}_2$  into the water column of large river systems are (1) in-situ respiration of organic material and (2) flushing of  $\text{CO}_2$  produced in soil pores from terrestrial and wetland environments via decomposition of organic material and root respiration [4]. The principal removal mechanism of aqueous  $\text{CO}_2$  is in-situ primary production, or photosynthesis [4]. Many of the world's largest rivers are supersaturated in  $\text{CO}_2$  with respect to the atmosphere, resulting in a large flux of  $\text{CO}_2$  from the water surface [1,5,6].

Current estimates of global  $\text{CO}_2$  flux from rivers to the atmosphere vary largely from 230 to 1800  $\text{Tg yr}^{-1}$  [2,3,7], calculated using partial pressure estimates of dissolved  $\text{CO}_2$  ( $p\text{CO}_2$ ), many of which are derived from low-time resolution (i.e., weekly or monthly) measurements of river alkalinity,

pH, and water temperature. This method of  $p\text{CO}_2$  calculation has been scrutinized for its great degree of uncertainty in temperate and tropical freshwaters due to the potential of significant contributions of organic acids to total alkalinity and low pH systems greatly over-estimating calculations [8]. The higher range of outgassing estimates is much greater than global estimates for the export of dissolved organic (200–360 Tg yr<sup>-1</sup>) and inorganic carbon (381–410 Tg yr<sup>-1</sup>), as well as particulate organic (180–240 Tg yr<sup>-1</sup>), and inorganic carbon (170 Tg yr<sup>-1</sup>) to the oceans [9–12]. Variation in estimates stem largely from differences in methods and data availability and resolution. One of the pioneering attempts in calculating total CO<sub>2</sub> outgassing from rivers by Cole and others [2] estimated 230 Tg yr<sup>-1</sup> based on data from approximately 80 rivers. Several years later, Raymond and others [3] estimated an annual outgassing of 1800 Tg yr<sup>-1</sup> from rivers, globally incorporating data collected from all stream orders with little requirements of data resolution. The most recent estimates by Lauerwald and others [7] excluded first order stream measurements and only included rivers with multiple samples collected across varying seasons, resulting in a global average riverine  $p\text{CO}_2$  value 700  $\mu\text{atm}$  less than Raymond et al. (i.e., 2400 vs. 3100  $\mu\text{atm}$ ) and an annual outgassing flux nearly one-third of the Raymond and others. Great strides have been made to improve freshwater CO<sub>2</sub> outgassing calculations and models through refining gas transfer velocities and  $p\text{CO}_2$  calculations based on regional hydrologic, climate, and atmospheric conditions. Yet, it is clear based on the large discrepancies in outgassing estimates stemming from the difference in spatial and temporal data resolution, that the lack of high resolution  $p\text{CO}_2$  data is a limiting factor on the accuracy of calculations.

Aquatic  $p\text{CO}_2$  can fluctuate both spatially and seasonally due to differences in land-use, discharge, water temperatures, and rates of biological respiration and photosynthesis [13–17]. Furthermore, aquatic respiration and photosynthesis rates can vary greatly over the span of a day due to a change in temperature and sunlight availability [18], resulting in a significant variability of  $p\text{CO}_2$  in water bodies between night and day [19–21]. A few recent studies have highlighted the importance of diel variation of  $p\text{CO}_2$  and CO<sub>2</sub> evasion from lakes and reservoirs. In a study conducted in Lochaber Lake in eastern Nova Scotia, Canada, Spafford and Risk [22] found that 65–95% of the total CO<sub>2</sub> release in a 24-h period occurred during the nocturnal period. From another reservoir study in Central Mississippi, USA, Liu et al. [23] reported that CO<sub>2</sub> effluxes at night were about 70% higher than those during the day. To date, this phenomenon has not been documented in a large, biologically productive river system. If the former theory is true for large rivers, it could have serious implications on the accuracy of calculating carbon budgets in freshwater systems, which are mostly based on low time-resolution measurements gathered during daylight hours.

In this study, we monitored hourly fluctuations of  $p\text{CO}_2$  in the surface water of the Lower Mississippi River and calculated hourly CO<sub>2</sub> outgassing over four 24-h periods in May and August 2018. The primary goal of this study was to identify whether a diel shift in  $p\text{CO}_2$  driven by solar radiation during the day results in significantly different  $p\text{CO}_2$  and CO<sub>2</sub> outgassing rates between daylight and darkness hours. The specific objectives of the study included (1) analyzing diel variability of  $p\text{CO}_2$  in the Lower Mississippi River; (2) estimating diel CO<sub>2</sub> outgassing with field measurements of  $p\text{CO}_2$ ; and (3) identifying environmental factors most influencing any notable diel variation. By achieving these objectives, we tested the hypothesis that riverine  $p\text{CO}_2$  will decrease over the span of daylight, likely due to a diel increase in photosynthesis driven by daytime surges in solar radiation and temperature. Likewise, riverine  $p\text{CO}_2$  should increase from sunset to dawn due to a net CO<sub>2</sub> input from river water respiration. This diel fluctuation of riverine  $p\text{CO}_2$  should cause a distinct daily cycle of riverine CO<sub>2</sub> outgassing, resulting in significantly higher outgassing rates during darkness hours.

## 2. Materials and Methods

This study was conducted in the Lower Mississippi River at Baton Rouge, Louisiana, USA (30°26′16.6″ N, 91°11′31.6″ W, Figure 1), approximately 369 river km upstream of the river's outlet to the Gulf of Mexico. The Mississippi is the largest river in North America, draining 3.2 million km<sup>2</sup> of land and discharging approximately 680 km<sup>3</sup> of freshwater into the Gulf annually, in combination with

the Atchafalaya River [24]. Due to the vast drainage size and diverse land use, the Mississippi River carries dissolved inorganic and organic carbon (DIC and DOC) from various sources, with an average DIC and DOC flux rate of  $12.6 \text{ Tg yr}^{-1}$  and  $4.1 \text{ Tg yr}^{-1}$ , respectively, at Baton Rouge during the past three years [25]. DIC fluxes over recent years are very similar to those reported in the Mississippi River at this location approximately one decade ago [26], however, recent DOC fluxes are nearly double some past estimates [27–29]. The large fluxes of diverse organic materials [30] and nutrients [31] provide the resources necessary for in-situ respiration, or production of  $\text{CO}_2$ . The river reach in our study area is approximately 750 m wide by 15 m deep, depending on the river stage, with a minimal slope [32], providing a slow-moving environment conducive of in-situ biological processing. The climate in southcentral Louisiana is considered subtropical, characterized by short, mild winters paired with humid, hot summer months. Based on these meteorological, physical, and biogeochemical characteristics of the river at our study site, we believe this portion of the river is biologically productive, especially as Dodds and others [33] found high rates of both in-situ photosynthesis and respiration in the river approximately 40 km downstream of our study site. We are only aware of one previous study [29] analyzing calculated  $p\text{CO}_2$  and  $\text{CO}_2$  outgassing values in the Lower Mississippi River, which suggested that the river was regularly super-saturated in  $p\text{CO}_2$  with respect to the atmosphere due to a combination of in-situ and terrestrial respiration of organic material. Two other studies [34,35] have reported a significant amount of carbon processing in the Lower Mississippi River's coastal plume near the river's mouth to the Gulf of Mexico.

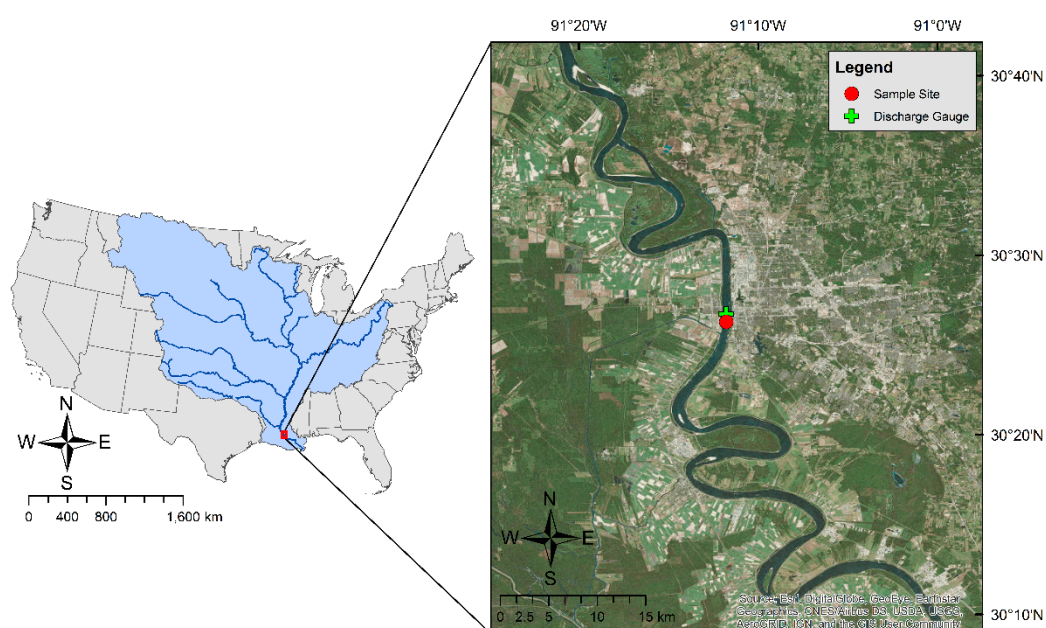


**Figure 1.** Mississippi River Basin with a vast drainage area of 3.2 million  $\text{km}^2$  and the locations of the sampling site and U.S. Geological Survey gauge station (USGS #07374000).

In May and August 2018, we conducted in-situ measurements at 3-h intervals over a span of 24 h starting at 6:00 Central Standard Time (CST) in the U.S. and ending on 6:00 CST the following day for two days in spring (11–12 May and 17–18 May) and two days in summer (13–14 August and 15–16 August). The field schedule was designed to capture high and low flow conditions as well as two different water temperature regimes, which typically occur in the Mississippi River during spring and summer months. During each field trip, in-situ measurements of partial pressure of carbon dioxide ( $p\text{CO}_2$ ) (C-Sense™  $p\text{CO}_2$  sensor, Turner Designs, San Jose, CA, USA), water temperature, dissolved oxygen (YSI 556 multi-probe meter, YSI Inc., Yellow, Springs, OH, USA), pH (Orion Star A221, Thermo Scientific, Beverly, MA, USA), and turbidity (T100, Oakton Instruments, Vernon Hills, IL, USA) were collected. The C-Sense™ measures  $p\text{CO}_2$  in-stream by gas diffusion across a hydrophobic

membrane into an isolated headspace chamber, where the wavelength of  $p\text{CO}_2$  is absorbed using infrared sensors. The sensor was calibrated at 20 °C at average sea-level atmospheric pressure less than six months prior to the field campaign using a manufacturer developed equation to convert sensor voltage output (V) to gaseous  $\text{CO}_2$  concentration (ppm). All  $p\text{CO}_2$  data are temperature corrected in real time, with a measurement range of 0–10,000  $\mu\text{atm}$  and 3% full scale accuracy. Both the C-Sense and YSI sensors equilibrated for 15 min and recorded for approximately 20 min during each sample, with the C-Sense collecting data every 30 s and the YSI every 5 s. Relevant atmospheric parameters, including hourly solar radiation, atmospheric temperature, and wind speed, were collected from the Louisiana State University Agricultural Center Ben Hur Research Station in Baton Rouge, LA (30°21'52" N, 91°10'02" W), located approximately 7 km southeast from the river sampling site. Solar radiation at Ben Hur Station is measured at the 400–1100 nm waveband interval using a LI200R-L pyranometer (Campbell Scientific, Logan, UT, USA). Hourly river discharge records of the Mississippi River at Baton Rouge were downloaded from the U.S. Geological Survey's gauging station, #07374000. These data built a foundation of ambient conditions for our  $p\text{CO}_2$  and  $\text{CO}_2$  outgassing analyses.

The flux of  $\text{CO}_2$ , or outgassing, between surface water and atmosphere ( $F\text{CO}_2$  in  $\text{mmol CO}_2 \text{ m}^{-2} \text{ h}^{-1}$ ) was calculated utilizing the following equation developed by Cai and Wang [36]:

$$F\text{CO}_2 = K_T K_H (p\text{CO}_{2\text{water}} - p\text{CO}_{2\text{air}}), \quad (1)$$

where  $K_T$  is the gas transfer velocity ( $\text{m d}^{-1}$ ),  $K_H$  is a solubility constant ( $\text{mol L}^{-1} \text{ atm}^{-1}$ ),  $p\text{CO}_{2\text{water}}$  is the partial pressure of dissolved  $\text{CO}_2$  in the water column ( $\mu\text{atm}$ ), and  $p\text{CO}_{2\text{air}}$  is the partial pressure of atmospheric  $\text{CO}_2$  ( $\mu\text{atm}$ ), which was fixed as 400  $\mu\text{atm}$  [37] for the study period. It is well understood that atmospheric  $\text{CO}_2$  can demonstrate diel variation on terrestrial land, yet the pattern of this variation can vary between and even within land-uses [38,39]. The nearest FLUXNET eddy covariance tower with atmospheric  $\text{CO}_2$  data is located several hundred kilometers from the study site and does not have data available for the study period. While using a fixed value does not account for any potential diel variation in atmospheric  $\text{CO}_2$ , applying diel variation found in an environment very different and far from the study area to our study area would introduce great uncertainty to the outgassing analysis. Additionally, a fixed atmospheric value is a widely-used method that reduces these assumptions and increases the ability to reproduce similar studies in the future, though the limitations of a fixed value should not be overlooked when considering the conclusions of this study. We selected a  $K_T$  value of  $4.3 \text{ m d}^{-1}$ , which is a rate lower than the global average of  $5.7 \text{ m d}^{-1}$  [3]; however, this has been reported as being more representative of large low-land rivers [3,40]. The solubility constant ( $K_H$ ) was calculated using the following equation by Weiss [41]:

$$\ln K_H = A_1 + A_2 \left( \frac{100}{T} \right) + A_3 \ln \left( \frac{100}{T} \right) + S \left[ B_1 + B_2 \left( \frac{T}{100} \right) + B_3 \left( \frac{T}{100} \right)^2 \right] \quad (2)$$

where  $A_1 = -58.0931$ ,  $A_2 = 90.5069$ ,  $A_3 = 22.2940$ ,  $B_1 = 0.027766$ ,  $B_2 = -0.025888$ ,  $B_3 = 0.0050578$ ,  $T$  is the absolute temperature of water in Kelvin, and  $S$  is the salinity. The study area is classified as a freshwater system; therefore, an  $S$  of 0 was used for calculating  $K_H$ . Daily  $\text{CO}_2$  outgassing ( $\text{mmol m}^{-2} \text{ d}^{-1}$ ) was calculated for each 24-h period using two difference methods. The first extrapolated the hourly flux rate at the 15:00 CST sample over the entire 24-h period. The second used linear interpolation to estimate hourly flux rates between 3-h sample intervals and then summed all hourly fluxes over the 24-h period.

Statistical analysis was conducted using SAS 9.2 software. Student's unpaired t-test was used to compare differences of means between seasons, samples within seasons, and samples experiencing solar radiation to those not. Only solar radiation readings during daylight hours were used to compare solar radiation between seasons and samples dates. Pearson correlation coefficients were calculated as a simple analysis of the relationships between  $p\text{CO}_2$ , ambient water parameters, and atmospheric parameters. An  $\alpha$  of 0.05 was used for all statistical analysis.

### 3. Results

#### 3.1. Hourly River Discharge, Water Conditions, and Atmospheric Measurements

During the study period, discharge in the Mississippi River at Baton Rouge (USGS #0774000) was three times greater in May ( $24,530 \text{ std.} \pm 1996 \text{ m}^3 \text{ s}^{-1}$ ) than in August ( $8912 \pm 57 \text{ m}^3 \text{ s}^{-1}$ ), which is representative of the typical long-term hydrograph of the river. Gathering samples over such a wide range of flow conditions allowed us to compare diel  $p\text{CO}_2$  dynamics under high and low flow regimes. In spring, river discharge marginally decreased over the diel period (Figure 2a). In summer river discharge remained constant over the 24-h samples.

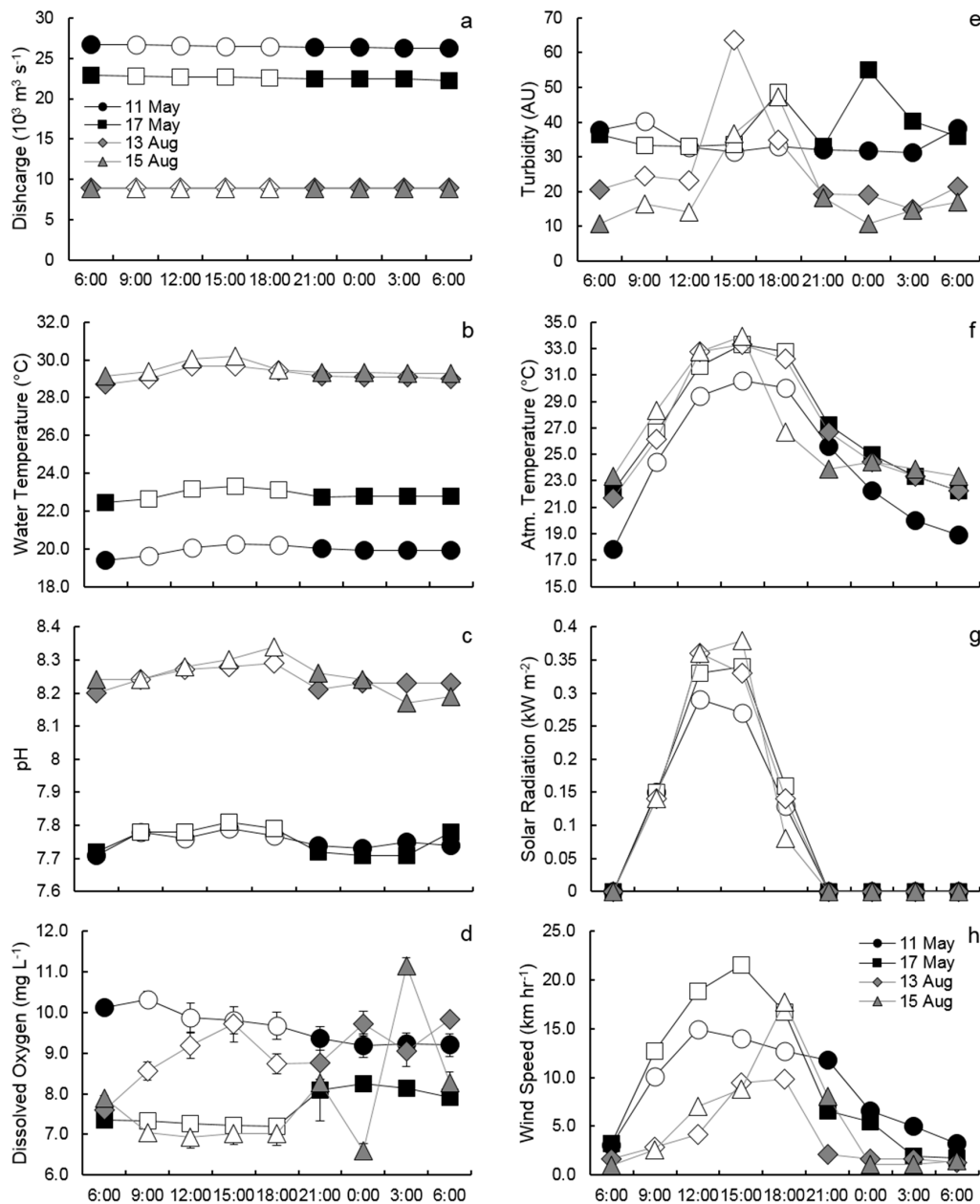


**Figure 2.** Diel variation of river discharge (a), water temperature (b), pH (c), dissolved oxygen (d), turbidity (e), atmospheric temperature (f), solar radiation (g), and wind speed (h) during the study period. Hollow data points represent samples collected during daylight hours (i.e., solar radiation  $>0.00 \text{ kW m}^{-2}$ ). The daily hours are Central Standard Time of the United States.

The magnitude of some ambient water parameters varied greatly between the seasons, however, diel variability was consistent between spring and summer. Water temperature was nearly 8 °C warmer in summer than spring, averaging 29.3 ( $\pm 0.4$ ) and 21.4 °C ( $\pm 1.5$ ), respectively. The pattern and degree of variability in water temperature was similar between all samples, with temperatures rising during daylight hours until 15:00 CST, gradually decreasing over the remainder of daylight, then remaining constant over evening hours (Figure 2b). Water temperatures on average varied by 0.9 °C ( $\pm 0.1$ ) over the 24-h periods, but demonstrated no significant difference between daylight and darkness hours. pH was also higher in summer than spring, averaging 7.75 ( $\pm 0.03$ ) in spring and 8.25 ( $\pm 0.04$ ) in summer. Diel variation in pH was similar to water temperature, with maximum measurements at 15:00 CST and lowest measurements during darkness hours (Figure 2c). pH varied on average by 0.09 ( $\pm 0.01$ ), resulting in measurements during daylight being significantly higher than during darkness ( $p < 0.0001$ ). DO averaged 8.64 ( $\pm 1.11$ ) in spring and 8.41 mg L<sup>-1</sup> ( $\pm 1.25$ ) in summer. The diel variability of DO was greater in summer, however, no clear diel pattern could be discerned (Figure 2d). Water turbidity was slightly higher in spring than summer, averaging 37 ( $\pm 6$ ) and 24 NTUs ( $\pm 14$ ), respectively. During the majority of sample periods, turbidity was highest during daylight hours (Figure 2e), likely due to daytime boat traffic in the river.

Meteorological parameters showed a minimal difference between spring and summer, but similar diel patterns between seasons. Air temperature averaged 25.7 °C ( $\pm 4.8$ ) in spring and 26.9  $\pm$  4.3 °C in summer. Diel variation in air temperature was consistent between samples, rising from sunrise until 15:00, where it then gradually decreased through to 6:00 the following day (Figure 2f). This distinct diel pattern resulted in an average diel temperature range of 11.3 °C ( $\pm 0.8$ ) and air temperatures significantly ( $p < 0.0001$ ) greater by 7.2 °C ( $\pm 2.7$ ) during daylight hours. Solar radiation did not vary between seasons, averaging 0.23 kW m<sup>-2</sup> ( $\pm 0.09$ ) in spring and 0.24 kW m<sup>-2</sup> ( $\pm 0.13$ ) in summer. During all sample days, solar radiation rose until 12:00 or 15:00 then decreased to 0 kW m<sup>-2</sup> by 21:00 (Figure 2g). Maximum solar radiation readings ranged between 0.27–0.38 kW m<sup>-2</sup>. Average wind speed was the only atmospheric parameter to reflect a large difference between seasons, with wind speeds on average two times higher in spring than summer (9.5  $\pm$  6.2 vs. 4.6  $\pm$  4.6 km hr<sup>-1</sup>). Wind speed in spring demonstrated a noticeable diel trend similar to solar radiation's diel curve, however, wind speed in summer slowly increased until 18:00 followed by a sharp decrease in the evening (Figure 2h). As a result, wind speed during daylight hours was significantly ( $p < 0.0001$ ) higher than during hours of darkness.

### 3.2. Diel pCO<sub>2</sub> Measurements

Mean pCO<sub>2</sub> during the study period was 1514  $\mu$ atm ( $\pm 652$ ), with all samples measuring greater than atmospheric CO<sub>2</sub> pressure (400  $\mu$ atm). Spring pCO<sub>2</sub> measurements were significantly ( $p < 0.0001$ ) higher than summer measurements, averaging 2140 ( $\pm 179$ ) and 888  $\mu$ atm ( $\pm 124$ ), respectively. There was no difference of means between summer measurements; however, mean pCO<sub>2</sub> was significantly ( $p = 0.0105$ ) higher on 17 May than on 11 May (2246  $\pm$  75 and 2033  $\pm$  192  $\mu$ atm, respectively). During all sample events, pCO<sub>2</sub> measurements were highest at 6:00 and lowest at 15:00 or 18:00 (Figure 3a,b). A diel trend was clear during all sample trips, with pCO<sub>2</sub> decreasing from 6:00 to 15:00 and gradually increasing from 15:00 to 6:00 the following day (Table 1).

In spring, pCO<sub>2</sub> levels dropped 9–18% from 6:00 to 15:00 and proceeded to rise 9–35% from 15:00 to 6:00 the following morning, demonstrating a diel range of 206–607  $\mu$ atm. The 17 May sample did not demonstrate as linear of a rise in pCO<sub>2</sub> in the evening hours as 11 May. The diel pattern was much more drastic in summer, dropping 33% from early morning to late afternoon and rising 35–55% until the following morning, resulting in a diel range between 344–377  $\mu$ atm. On the morning of 13 August, pCO<sub>2</sub> dropped until 12:00, rather than 15:00, and remained at a fairly consistent level until the 21:00 sample, resulting in not as strong of fit in our model (Table 1). This diel pattern resulted in summer pCO<sub>2</sub> measurements 25% (std.  $\pm$  10%) greater during darkness hours than daylight hours (Figure 4a). Spring darkness pCO<sub>2</sub> measurements were on average 7% ( $\pm 8\%$ ) greater than daylight measurements.

These results partially affirm our hypothesis that  $p\text{CO}_2$  is noticeably lower during daylight hours due to a diel pattern.

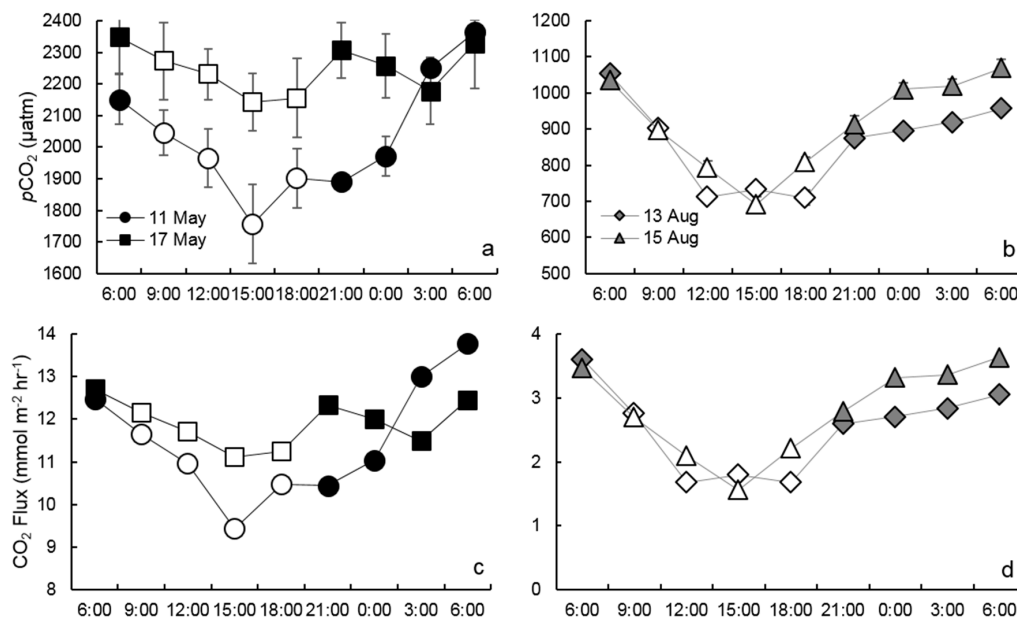


**Figure 3.** Daily variation in  $p\text{CO}_2$  (a,b) and  $\text{CO}_2$  flux (c,d) in the Lower Mississippi River during spring (a,c) and fall (b,d). Data points in (a) and (b) represent the mean  $p\text{CO}_2$  value and error bars represent the standard deviation of the respective samples. The hollow data points represent samples collected during daylight hours (i.e., solar radiation > 0.00  $\text{kW m}^{-2}$ ). The daily hours are Central Standard Time of the United States.

**Table 1.** Linear regressions of  $p\text{CO}_2$  and  $\text{CO}_2$  flux ( $\text{mmol m}^{-2} \text{h}^{-1}$ ) with hourly time steps (H) for 6:00 to 15:00 (Morning) and for 15:00 to 6:00 the following day (Evening). For example, “6:00” corresponds to “6” in the model. For 0:00, 3:00, and 6:00 the following day, the values 24, 27, and 30 were used. Statistical significance level  $\alpha = 0.05$ .

Date	Morning	$R^2$ ( $p$ -Value)	Evening	$R^2$ ( $p$ -Value)
11 May	$p\text{CO}_2 = -42.14H + 2421$	0.95 (0.0009)	$p\text{CO}_2 = 39.67H + 1130$	0.90 (0.0036)
17 May	$p\text{CO}_2 = -21.99H + 2479$	0.98 (0.0081)	$p\text{CO}_2 = 9.016H + 2025$	0.40 (0.1782)
13 Aug	$p\text{CO}_2 = -38.54H + 1254$	0.86 (0.0709)	$p\text{CO}_2 = 16.93H + 467.0$	0.86 (0.0081)
15 Aug	$p\text{CO}_2 = -37.78H + 1250$	0.99 (0.0033)	$p\text{CO}_2 = 24.96H + 357.1$	0.93 (0.0018)
11 May	$\text{FCO}_2 = -0.3285H + 14.58$	0.97 (0.0010)	$\text{FCO}_2 = 0.2859H + 4.923$	0.91 (0.0028)
17 May	$\text{FCO}_2 = -0.1767H + 13.78$	0.99 (0.0016)	$\text{FCO}_2 = 0.06883H + 10.22$	0.45 (0.1434)
13 Aug	$\text{FCO}_2 = -0.2178H + 4.743$	0.86 (0.0700)	$\text{FCO}_2 = 0.09467H + 0.3138$	0.86 (0.0077)
15 Aug	$\text{FCO}_2 = -0.2113H + 4.668$	0.99 (0.0037)	$\text{FCO}_2 = 0.1379H - 0.2888$	0.93 (0.0018)

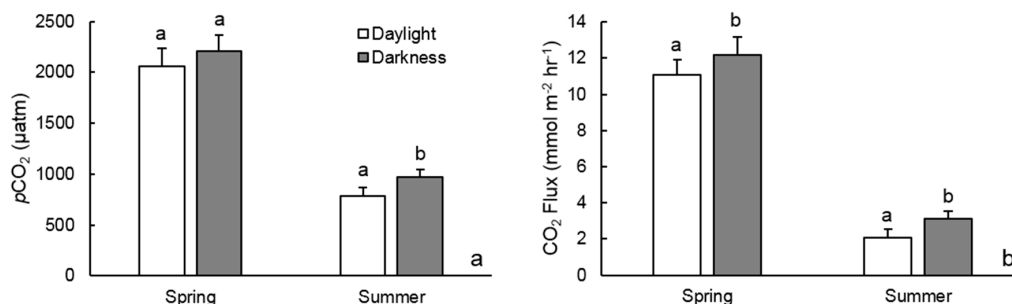


**Figure 4.** Mean  $p\text{CO}_2$  (a) and  $\text{CO}_2$  (b) outgassing rates during darkness and daylight hours by season. Bar pairs with different letters above them represent a significant difference between populations at  $\alpha = 0.05$ . Error bars represent standard deviations.

### 3.3. CO<sub>2</sub> Outgassing Estimates

Estimated rates of CO<sub>2</sub> outgassing averaged 7.2 mmol m<sup>-2</sup> h<sup>-1</sup> (±4.7) during the study period. Outgassing rates were significantly ( $p < 0.0001$ ) higher in the spring than summer, averaging 11.7 (±1.1) and 2.7 (±0.7) mmol m<sup>-2</sup> h<sup>-1</sup>, respectively. There was no significant difference in CO<sub>2</sub> outgassing between samples in the same season. Similar to *p*CO<sub>2</sub>, diel variability in CO<sub>2</sub> outgassing reflected a clear trend in both seasons (Figure 3c,d), decreasing from 6:00 to 15:00 and gradually increasing from 15:00 to 6:00 the following day (Table 1). In spring, outgassing rates gradually decreased by 13–24% from 6:00 to 15:00, followed by an increase of 12–46% until 6:00 the following day. Spring rates ranged by 1.5–4.4 mmol m<sup>-2</sup> h<sup>-1</sup> over a 24-h period. Much sharper diel increases and decreases occurred in the summer samples. CO<sub>2</sub> outgassing rates decreased by 54% from 6:00 to 12:00 on 13 August and by 55% from 6:00 to 15:00 on 15 August. Summer afternoon outgassing rates increased by 65–82% (1.4–2.1 mmol m<sup>-2</sup> h<sup>-1</sup>) from their respective minimums until 6:00 the following morning. This trend resulted in a summer diel range of 1.9–2.2 mmol m<sup>-2</sup> h<sup>-1</sup>. Consequently, CO<sub>2</sub> outgassing rates during hours of darkness were significantly ( $p < 0.0001$ ) greater than daylight in both seasons (Figure 4b). Spring outgassing rates during darkness were on average 10% (std. ±8%) higher than during daylight hours, while darkness rates in summer were on average 25% (±10%) greater. Calculating daily outgassing (mmol m<sup>-2</sup> d<sup>-1</sup>) for sample days using linear interpolation between the 3-h intervals, rather than extrapolating the 15:00 measurement across the entire 24-h period, resulted in significantly higher daily outgassing rates in a paired t-test ( $p = 0.0261$ ), ranging between 15.3 and 43.6 (mean 26.2, std. ±12.7 mmol m<sup>-2</sup> d<sup>-1</sup>) higher than the single measurement calculation (Figure 5). These results strongly support our initial hypothesis.

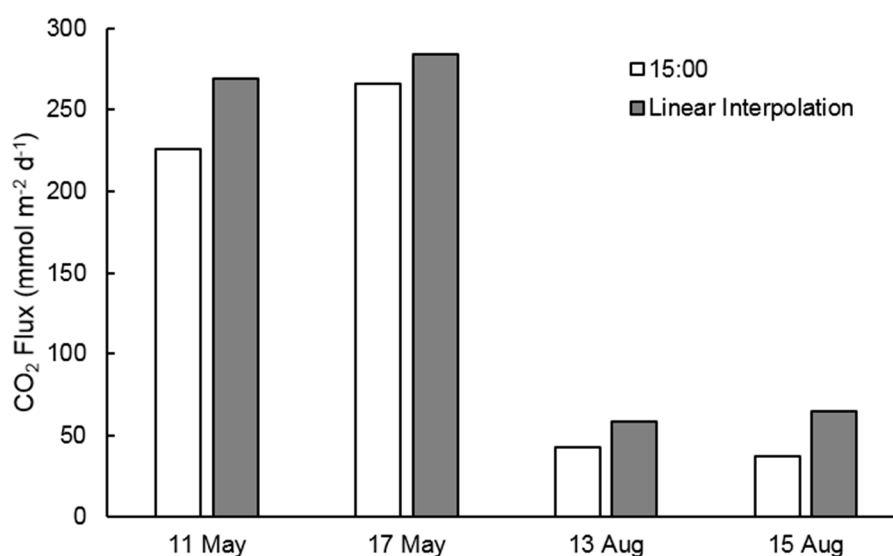


**Figure 5.** Comparison of daily outgassing calculations. “15:00” data represents extrapolating CO<sub>2</sub> flux rates at 15:00 CST over the 24-h period. “Linear Interpolation” data represents daily flux calculated by linear interpolation between 3-h intervals.

## 4. Discussion

### 4.1. Seasonal *p*CO<sub>2</sub> Differences

The difference in riverine *p*CO<sub>2</sub> between seasons can likely be explained by comparing the difference in ambient water and atmospheric parameters between seasons and analyzing their relationships with *p*CO<sub>2</sub>. *p*CO<sub>2</sub> demonstrated positive correlations with river discharge and turbidity and inverse relationships with water temperature and pH (Table 2).

**Table 2.** Pearson correlation coefficients among  $p\text{CO}_2$ , water temperature ( $T_w$ ), dissolved oxygen (DO), pH, turbidity (N), atmospheric temperature ( $T_a$ ), wind speed (u), solar radiation (SR), and river discharge (Q). Only significant correlations at  $\alpha = 0.05$  are shown.

	$p\text{CO}_2$	$T_w$	DO	pH	N	$T_a$	u	SR	Q
$p\text{CO}_2$	1.00	−0.92	-	−0.98	0.46	-	-	-	0.93
$T_w$		1.00	-	0.96	−0.46	-	-	-	−0.99
DO			1.00	-	-	-	-	-	-
pH				1.00	−0.47	-	-	0.76	−0.97
N					1.00	-	0.48	-	0.49
$T_a$						1.00	0.63	0.86	-
u							1.00	0.60	0.40
SR								1.00	-
Q									1.00

We postulate the difference in  $p\text{CO}_2$  between seasons is primarily driven by two processes regulated by river discharge. First, the dissolution of soil pore-water  $\text{CO}_2$  during the spring high-flow period caused higher  $p\text{CO}_2$  levels in spring than summer. As soils become wetted and their temperatures begin to rise in spring months, conditions become more favorable for  $\text{CO}_2$  producing microbial processes as found by Hope et al [42], resulting in soil  $p\text{CO}_2$  concentrations generally much greater than atmospheric  $p\text{CO}_2$  [43]. The flushing of soil  $p\text{CO}_2$  into rivers via baseflow and interflow has been documented by Richey et al. [4] as a significant piece of the riverine  $\text{CO}_2$  cycle. Second, the respiration of organic material delivered to the river during the spring high-flow period likely resulted in higher  $p\text{CO}_2$  values. Organic carbon concentrations and community respiration are strongly correlated with discharge in the Mississippi River, which in-turn correlate with the greater production of  $p\text{CO}_2$  and greater net heterotrophy in spring [26,33]. Despite a slower river flow velocity, greater water temperatures, and lower turbidity in summer providing an environment more conducive of biological processing [44], the lack of organic inputs associated with lower discharge likely limited  $p\text{CO}_2$  production, resulting in a greater net removal of  $p\text{CO}_2$ . This phenomenon is reflected in significantly higher pH in the river during the summer and the inverse relationship between  $p\text{CO}_2$  and river pH (Table 2).

#### 4.2. Biological Processes Influencing Diel $p\text{CO}_2$ Variation

This is the first study to document significant diel variation of riverine  $p\text{CO}_2$  and  $\text{CO}_2$  outgassing utilizing actual in-stream measurements in the Lower Mississippi River. These findings are in coincidence with studies that have found a similar pattern of a reduction of atmospheric  $\text{CO}_2$  over large water bodies during daylight hours [45,46] This variation is apparently driven by autotrophic processes, resulting in an increase in net ecosystem production (NEP = gross primary production (GPP)—community respiration (CR)) [47] over daylight hours. During all samples across both seasons,  $p\text{CO}_2$  values were highest during the dark, early morning hours and lowest between 15–18:00 CST, following the peak of daylight (Figure 3a,b). The large variation suggests a diel change in the balance of processes producing and removing  $p\text{CO}_2$  in the water column. Reduction in  $p\text{CO}_2$  over daylight corresponded with a diel increase in water temperature and solar radiation (Figure 2b,g), both of which have shown to increase aquatic metabolism [48,49]. The decrease in  $p\text{CO}_2$  also paired with an increase in pH over daylight hours (Figure 2c). This relationship suggests a diel increase in photosynthesis may be driving the decrease in  $p\text{CO}_2$  as in-situ photosynthesis would drive up pH values. Our in-stream measurements confirm results of a past study of diel  $p\text{CO}_2$  dynamics and stream metabolism in two acidic lower-order peatland streams by Dawson et al. [50], which found lowest  $p\text{CO}_2$  levels during early afternoon hours, highest values in the early morning, and a diel increase in NEP, especially during warmer months. In a separate study of aquatic metabolism, Mulholland and others [47] also documented a diel increase in NEP in many of the streams studied due to a daily increase in GPP, but fairly consistent CR rates. The authors concluded the shift in NEP was driven primarily by

solar radiation rather than water temperature. We hypothesize that the diel variation in  $p\text{CO}_2$  in the Mississippi River can be explained by a similar shift in NEP, likely controlled by solar radiation driving up photosynthesis rates, as recent studies in the Mississippi and Chattahoochee Rivers have found that water temperature is not a strong predictor of GPP in either river [33]. Even though  $p\text{CO}_2$  values were significantly lower during daylight hours in this study, water temperature showed minimal difference between daylight and darkness, suggesting that a minor shift in water temperature is not the main driver of diel variability.

The diel decrease in  $p\text{CO}_2$  was in coincidence with a diel increase in average wind speed during all sample events (Figure 2h). Some studies [15,40] found that an increase in wind speed can speed up the rate of  $p\text{CO}_2$  lost to the atmosphere, especially in large bodies of water, by directly increasing the gas transfer velocity of  $\text{CO}_2$ . Wind can increase gas transfer velocity due mainly to creating surface water turbulence in stagnant water [51], which may, however, not be relevant for a large flowing river like the Mississippi River, that consistently experiences water turbulence. Also, if wind were the main factor driving variation, we would have anticipated a larger diel decrease in  $p\text{CO}_2$  on days when wind speeds were greatest. Yet, we found the lowest variation in  $p\text{CO}_2$  on 17 May when the average wind speed was highest (see the low  $\beta_1$  values in Table 1). Based on the findings by Schubert and Forster [52] and Helbling et al. [53], an increase in wind speed could also increase the velocity of water column mixing, indirectly inhibiting photosynthesis in primary producers near the surface of the water column. Based on these findings, it is unclear whether wind speed has a significant influence on diel  $p\text{CO}_2$  variability.

Diel fixation of  $\text{CO}_2$  by aquatic plants is another potential removal mechanism in the water column, especially in  $\text{CO}_2$  saturated waters [54]. Rich and others [55] studied photosynthesis of submerged aquatic vegetation at the diel scale in a pond and found that water column oxygen production and pH increased with solar radiation, while water column  $p\text{CO}_2$  decreased. Additional past studies have found light availability as one of the most important factors limiting daily aquatic plant photosynthesis [56,57], suggesting potential for a diel  $\text{CO}_2$  cycling due to photosynthesis. However, the levees of the Lower Mississippi through the study area are heavily industrialized and the river channel is regularly dredged for large freight ships, highly limiting the growth of natural vegetation. As a result, diel photosynthesis of aquatic plants is likely not a primary contributor to the diel  $\text{CO}_2$  cycling in the water-column found in this study, however, this process could have a significant impact in vegetation rich streams.

#### 4.3. Implications for Carbon Outgassing Estimates and Future Research Needs

This study found  $\text{CO}_2$  outgassing rates significantly lower during daylight hours in spring and summer, resulting in a large underestimation of daily outgassing rates under varying flow and temperature regimes. As GPP is generally highest in the Mississippi River in autumn and winter months [33], we would anticipate a similar diel trend throughout these seasons. Though diel variation may not be as drastic in autumn and winter due to lower temperatures, shorter day-light lengths, and potential nutrient limitations [58]. These findings raise questions about the current global estimation of  $\text{CO}_2$  outgassed from rivers. Assuming a 34% under-estimation of a total flux of  $650 \text{ Tg C yr}^{-1}$ , as recently calculated by Lauerwald and others [7], would result in an under-estimation of  $221 \text{ Tg C}$  outgassed from streams and rivers to the atmosphere, annually. However, it should be noted that many large tropical rivers that contribute significantly to fresh-water  $\text{CO}_2$  emissions [59,60] may not experience this large of a diel cycle due to limited light attenuation and low nutrient levels limiting GPP [61,62], limiting the applications of this analysis. Nonetheless, several major world rivers have biogeochemical trends similar to the Mississippi River and diel variability may be even higher in other rivers depending on climate, nutrient, and organic matter availability, and varying day-night length ratios across geographic regions. Therefore, we argue that future high-resolution sampling studies analyzing diel  $p\text{CO}_2$  and  $\text{CO}_2$  outgassing dynamics in rivers at differing orders and varying latitudes would be beneficial for constraining the relationship between diel variability and the former

environmental factors. Ideally, these relationships could be used to develop a collective day-night  $p\text{CO}_2$  curve that could be used to incorporate diel variability in global  $\text{CO}_2$  outgassing estimations.

The large range of values in global outgassing estimates highlights the need of high-resolution in-stream samples. High resolution sampling would not only constrain the diel variation found in this study, but also incorporate seasonal and spatial variation found in several past studies [12–16,45]. It is clear that the estimation of  $\text{CO}_2$  outgassing has continued to increase as more data has been collected across rivers at varying orders and geographic locations, shifting the paradigm of the river's role in the carbon cycle. Estimates by Raymond and others [3] was the only study to include first-order streams, but was responsible for noting the very high  $p\text{CO}_2$  values with low data resolution, which likely skewed their estimates of  $1800 \text{ Tg yr}^{-1}$ . Therefore, conducting high-resolution sampling similar to that conducted in this study in varying geographic regions, as well as in lower order streams and along spatial gradients in large river systems, could help constrain concerns regarding the uncertainties in  $p\text{CO}_2$  measurements driving variability in outgassing calculations from aquatic systems.

## 5. Conclusions

This study monitored in-stream  $p\text{CO}_2$  and ambient water and weather conditions in spring and summer of 2018 in the Lower Mississippi River under varying river discharge and temperature regimes. Based on the field measurements at 3-h intervals, hourly  $\text{CO}_2$  outgassing rates for this 10th-order, large river system were estimated. The ultimate goal of the study was to assess the diel riverine  $p\text{CO}_2$  cycle and its influence on  $\text{CO}_2$  outgassing calculations. To our best knowledge, this is the first field assessment on diel  $p\text{CO}_2$  and  $\text{CO}_2$  emissions from a large river, and the findings may have important implications for constraining the uncertainty of river  $\text{CO}_2$  outgassing estimates. Seasonally, we found significantly higher  $p\text{CO}_2$  values and  $\text{CO}_2$  outgassing rates in spring than in summer, likely due to the higher input of carbon sources from river discharge. On a daily basis in the two seasons, both riverine  $p\text{CO}_2$  and  $\text{CO}_2$  outgassing showed a distinct diel cycle, with levels decreasing from sunrise to peak daylight hours, followed by a gradual increase during hours of darkness.  $p\text{CO}_2$  measurements varied by  $206\text{--}607 \mu\text{atm}$  over 24-h periods with significantly lower  $p\text{CO}_2$  values during daylight hours in summer.  $\text{CO}_2$  flux rates ranged by  $1.5\text{--}4.4 \text{ mmol m}^{-2} \text{ h}^{-1}$  over the 24-h periods, with outgassing rates significantly lower during daylight hours in both seasons. Incorporating diel variation in daily  $\text{CO}_2$  outgassing calculations resulted in outgassing rates  $26.2 \text{ mmol m}^{-2} \text{ d}^{-1}$  ( $\pm \text{std. } 12.7$ ) greater than calculations using a single daily  $p\text{CO}_2$  measurement. Diel decreases in  $p\text{CO}_2$  corresponded closely with increasing solar radiation and pH, suggesting strong autotrophic processes regulating  $\text{CO}_2$  levels in this large river system as we initially hypothesized. As many outgassing calculations are based on low-resolution samples collected during daylight hours, we postulate that many river  $\text{CO}_2$  emission estimates are likely underestimated. In order to constrain this uncertainty, future research utilizing high resolution  $p\text{CO}_2$  measurements in streams spanning differing orders, geographic regions, and biological communities is needed.

**Author Contributions:** Y.J.X. conceived and designed the study; J.H.R. performed the field sampling, measurements and data analysis; J.H.R. and Y.J.X. wrote and revised the manuscript.

**Funding:** This study was primarily supported through a National Fish and Wildlife Foundation grant (Project#: 8004.12.036402). The study was also supported from a U.S. Department of Agriculture Hatch Fund grant (Project#: LAB94230).

**Acknowledgments:** The authors are grateful to the U.S. Geological Survey for providing river discharge data and the Louisiana State University Agricultural Center Ben Hur Research Station for providing meteorological records. The authors also extend a thank you to undergraduate research assistant Skylar Bueche for her assistance with field data collection, as well as to six anonymous reviewers for their helpful comments and suggestion.

**Conflicts of Interest:** The authors declare no conflict of interest.

## References

1. Butman, D.; Raymond, P.A. Significant efflux of carbon dioxide from streams and rivers in the United States. *Nat. Geosci.* **2011**, *4*, 839–842. [[CrossRef](#)]
2. Cole, J.J.; Caraco, N.F. Carbon in catchments: Connecting terrestrial carbon losses with aquatic metabolism. *Mar. Freshw. Res.* **2001**, *52*, 101–110. [[CrossRef](#)]
3. Raymond, P.A.; Hartmann, J.; Lauerwald, R.; Sobek, S.; McDonald, C.; Hoover, M.; Butman, D.; Striegl, R.; Mayorga, E.; Humborg, C.; et al. Global carbon dioxide emissions from inland waters. *Nature* **2013**, *503*, 355–359. [[CrossRef](#)] [[PubMed](#)]
4. Richey, J.E. Pathways of atmospheric CO<sub>2</sub> through fluvial systems. In *Scientific Committee on Problems of the Environment (SCOPE)/United Nations Environment Programme (UNEP)—The Global Carbon Cycle: Integrating Humans, Climate, and the Natural World*; Island Press: Washington, DC, USA, 2013.
5. Richey, J.E.; Melack, J.M.; Aufdenkampe, A.K.; Ballester, V.M.; Hess, L.L. Outgassing from Amazonian rivers and wetlands as a large tropical source of atmospheric CO<sub>2</sub>. *Nature* **2002**, *416*, 617–620. [[CrossRef](#)] [[PubMed](#)]
6. Ran, L.; Lu, X.X.; Richey, J.E.; Sun, H.; Han, J.; Yu, R.; Liao, S.; Yi, Q. Long-term spatial and temporal variation of CO<sub>2</sub> partial pressure in the Yellow River, China. *Biogeosciences* **2015**, *12*, 921–932. [[CrossRef](#)]
7. Lauerwald, R.; Laruelle, G.G.; Hartmann, J.; Ciais, P.; Regnier, P.A.G. Spatial patterns in CO<sub>2</sub> evasion from the global river network. *Glob. Biogeochem. Cycles* **2015**, *29*, 534–554. [[CrossRef](#)]
8. Abril, G.; Bouillon, S.; Darchambeau, F.; Teodoru, C.R.; Marwick, T.R.; Tammooh, F.; Ochieng Omengo, F.; Geeraert, N.; Deirmendjian, L.; Polsenaere, P.; et al. Technical Note: Large overestimation of pCO<sub>2</sub> calculated from pH and alkalinity in acidic, organic-rich freshwaters. *Biogeosciences* **2015**, *12*, 67–78. [[CrossRef](#)]
9. Meybeck, M. Carbon, nitrogen, and phosphorus transport by world rivers. *Am. J. Sci.* **1982**, *282*, 401–450. [[CrossRef](#)]
10. Meybeck, M. Riverine transport of atmospheric carbon—sources, global typology and budget. *Water Air Soil Pollut.* **1993**, *70*, 443–463. [[CrossRef](#)]
11. Aitkenhead, J.A.; McDowell, W.H. Soil C:N ratio as a predictor of annual riverine DOC flux at local and global scales. *Glob. Biogeochem. Cycles* **2000**, *14*, 127–138. [[CrossRef](#)]
12. Li, M.; Peng, C.; Wang, M.; Xue, W.; Zhang, K.; Wang, K.; Shi, G.; Zhu, Q. The carbon flux of global rivers: A re-evaluation of amount and spatial patterns. *Ecol. Indic.* **2017**, *80*, 40–51. [[CrossRef](#)]
13. Hélie, J.-F.; Hillaire-Marcel, C.; Rondeau, B. Seasonal changes in sources and fluxes of dissolved inorganic carbon through the St. Lawrence River—Isotopic and chemical constraint. *Chem. Geol.* **2002**, *186*, 117–138. [[CrossRef](#)]
14. Ran, L.; Lu, X.X.; Liu, S. Dynamics of riverine CO<sub>2</sub> in the Yangtze River fluvial network and their implications for carbon evasion. *Biogeosciences* **2017**, *14*, 2183–2198. [[CrossRef](#)]
15. Raymond, P.A.; Caraco, N.F.; Cole, J.J. Carbon dioxide concentration and atmospheric flux in the Hudson River. *Estuaries* **1997**, *20*, 381–390. [[CrossRef](#)]
16. Zhang, L.; Xue, M.; Wang, M.; Cai, W.-J.; Wang, L.; Yu, Z. The spatiotemporal distribution of dissolved inorganic and organic carbon in the main stem of the Changjiang (Yangtze) River and the effect of the Three Gorges Reservoir. *J. Geophys. Res. Biogeosci.* **2014**, *119*, 741–757. [[CrossRef](#)]
17. Borges, A.V.; Darchambeau, F.; Lambert, T.; Bouillon, S.; Morana, C.; Brouyère, S.; Hakoun, V.; Jurado, A.; Tseng, H.C.; Descy, J.P.; et al. Effects of agricultural land use on fluvial carbon dioxide, methane and nitrous oxide concentrations in a large European river, the Meuse (Belgium). *Sci. Total Environ.* **2018**, *610–611*, 342–355. [[CrossRef](#)] [[PubMed](#)]
18. Falkowski, P.G.; Raven, J.A. *Aquatic Photosynthesis*, 2nd ed.; Princeton University Press: Princeton, NJ, USA, 2007.
19. Lynch, J.K.; Beatty, C.M.; Seidel, M.P.; Jungst, L.J.; DeGrandpre, M.D. Controls of riverine CO<sub>2</sub> over an annual cycle determined using direct, high temporal resolution pCO<sub>2</sub> measurements. *J. Geophys. Res.* **2010**, *115*. [[CrossRef](#)]
20. Yang, R.; Chen, B.; Liu, H.; Liu, Z.; Yan, H. Carbon sequestration and decreased CO<sub>2</sub> emission caused by terrestrial aquatic photosynthesis: Insights from diel hydrochemical variations in an epikarst spring and two spring-fed ponds in different seasons. *Appl. Geochem.* **2015**, *63*, 248–260. [[CrossRef](#)]

21. Yates, K.K.; Dufore, C.; Smiley, N.; Jackson, C.; Halley, R.B. Diurnal variation of oxygen and carbonate system parameters in Tampa Bay and Florida Bay. *Mar. Chem.* **2007**, *104*, 110–124. [[CrossRef](#)]
22. Spafford, L.; Risk, D. Spatiotemporal Variability in Lake-Atmosphere Net CO<sub>2</sub> Exchange in the Littoral Zone of an Oligotrophic Lake. *J. Geophys. Res. Biogeosci.* **2018**, *123*, 1260–1276. [[CrossRef](#)]
23. Liu, H.P.; Zhang, Q.Y.; Katul, G.G.; Cole, J.J.; Chapin, F.S.; MacIntyre, S. Large CO<sub>2</sub> effluxes at night and during synoptic weather events significantly contribute to CO<sub>2</sub> emissions from a reservoir. *Environ. Res. Lett.* **2016**, *11*, 8. [[CrossRef](#)]
24. Xu, Y.J.; DelDuco, E.M. Unravelling the relative contribution of dissolved carbon by the Red River to the Atchafalaya River. *Water* **2017**, *9*, 871. [[CrossRef](#)]
25. Reiman, J.R.; Xu, Y.J. A recent update in carbon transport: The Mississippi-Atchafalaya River System. In Proceedings of the 2018 State of the Coast Conference, New Orleans, LA, USA, 30 May–1 June 2018. [[CrossRef](#)]
26. Cai, Y.H.; Guo, L.D.; Wang, X.R.; Aiken, G. Abundance, stable isotopic composition, and export fluxes of DOC, POC, and DIC from the Lower Mississippi River during 2006–2008. *J. Geophys. Res. Biogeosci.* **2015**, *120*, 2273–2288. [[CrossRef](#)]
27. Ren, W.; Tian, H.; Cai, W.-J.; Lohrenz, S.E.; Hopkinson, C.S.; Huang, W.-J.; Yang, J.; Tao, B.; Pan, S.; He, R. Century-long increasing trend and variability of dissolved organic carbon export from the Mississippi River basin driven by natural and anthropogenic forcing. *Glob. Biogeochem. Cycles* **2016**, *30*, 1288–1299. [[CrossRef](#)]
28. Bianchi, T.S.; Wysocki, L.A.; Stewart, M.; Filley, T.R.; McKee, B.A. Temporal variability in terrestrially-derived sources of particulate organic carbon in the lower Mississippi River and its upper tributaries. *Geochim. Cosmochim. Acta* **2007**, *71*, 4425–4437. [[CrossRef](#)]
29. Dubois, K.D.; Lee, D.; Veizer, J. Isotopic constraints on alkalinity, dissolved organic carbon, and atmospheric carbon dioxide fluxes in the Mississippi River. *J. Geophys. Res. Biogeosci.* **2010**, *115*, 2156–2202. [[CrossRef](#)]
30. Shen, Y.; Fichot, C.G.; Benner, R. Floodplain influence on dissolved organic matter composition and export from the Mississippi-Atchafalaya River system to the Gulf of Mexico. *Limnol. Oceanogr.* **2012**, *57*, 1149–1160. [[CrossRef](#)]
31. BryantMason, A.; Xu, Y.J.; Altabet, M. Isotopic signature of nitrate in river waters of the lower Mississippi and its distributary, the Atchafalaya. *Hydrol. Process.* **2013**, *27*, 2840–2850. [[CrossRef](#)]
32. USACE. *The 2013 Mississippi River Hydrographic Survey Book*; U.S. Army Corps of Engineers District: New Orleans, LA, USA, 2013; p. 91. Available online: [http://www.mvn.usace.army.mil/Portals/56/docs/engineering/Geospatial/MRHB\\_2013/PDF/MRHB\\_2013.pdf](http://www.mvn.usace.army.mil/Portals/56/docs/engineering/Geospatial/MRHB_2013/PDF/MRHB_2013.pdf) (accessed on 5 November 2018).
33. Dodds, W.K.; Veach, A.M.; Ruffing, C.M.; Larson, D.M.; Fischer, J.L.; Costigan, K.H. Abiotic controls and temporal variability of river metabolism: Multiyear analyses of Mississippi and Chattahoochee River data. *Freshw. Sci.* **2013**, *32*, 1073–1087. [[CrossRef](#)]
34. Green, R.F.; Bianchi, T.S.; Dagg, M.J.; Walker, N.D.; Breed, G.A. An organic carbon budget for the Mississippi River turbidity plume and plume contributions to air-sea CO<sub>2</sub> fluxes and bottom water hypoxia. *Estuaries Coasts* **2006**, *29*, 579–597. [[CrossRef](#)]
35. Guo, X.; Cai, W.-J.; Huang, W.-J.; Wang, Y.; Chen, F.; Murrell, M.C.; Lohrenz, S.E.; Jiang, L.-Q.; Dai, M.; Hartmann, J.; et al. Carbon dynamics and community production in the Mississippi River plume. *Limnol. Oceanogr.* **2012**, *57*, 1–17. [[CrossRef](#)]
36. Cai, W.-J.; Wang, Y. The chemistry, fluxes, and sources of carbon dioxide in the estuarine waters of the Satilla and Altamaha Rivers, Georgia. *Limnol. Oceanogr.* **1998**, *43*, 657–668. [[CrossRef](#)]
37. National Ocean & Atmospheric Administration Earth System Research Laboratory Global Monitoring Division Website. Available online: <https://www.esrl.noaa.gov/gmd/ccgg/trends/data.html> (accessed on 12 June 2018).
38. Ward, H.C.; Kotthaus, S.; Grimmond, C.S.; BJORKEGREN, A.; Wilkinson, M.; Morrison, W.T.; Evans, J.G.; Morison, J.I.; Iamarino, M. Effects of urban density on carbon dioxide exchanges: Observations of dense urban, suburban and woodland areas of southern England. *Environ. Pollut.* **2015**, *198*, 186–200. [[CrossRef](#)] [[PubMed](#)]
39. Imasu, R.; Tanabe, Y. Diurnal and seasonal variations of carbon dioxide (CO<sub>2</sub>) concentrations in urban, suburban, and rural areas around Tokyo. *Atmosphere* **2018**, *9*, 367. [[CrossRef](#)]

40. Alin, S.R.; de Fátima, F.L.; Rasera, M.; Salimon, C.I.; Richey, J.E.; Holtgrieve, G.W.; Krusche, A.V.; Snidvongs, A. Physical controls on carbon dioxide transfer velocity and flux in low-gradient river systems and implications for regional carbon budgets. *J. Geophys. Res. Biogeosci.* **2011**, *116*. [[CrossRef](#)]
41. Weiss, R.F. Carbon dioxide in water and seawater: The solubility of a non-ideal gas. *Mar. Chem.* **1974**, *2*, 203–215. [[CrossRef](#)]
42. Hope, D.; Palmer, S.M.; Billett, M.F.; Dawson, J.J.C. Variations in dissolved CO<sub>2</sub> and CH<sub>4</sub> in a first-order stream and catchment: An investigation of soil-stream linkages. *Hydrol. Process.* **2004**, *18*, 3255–3275. [[CrossRef](#)]
43. Finlay, J.C. Controls of streamwater dissolved inorganic carbon dynamics in a forested watershed. *Biogeochemistry* **2003**, *62*, 231–252. [[CrossRef](#)]
44. Barth, J.A.; Veizer, J. Carbon cycle in St. Lawrence aquatic ecosystems at Cornwall (Ontario), Canada: Seasonal and spatial variations. *Chem. Geol.* **1999**, *159*, 107–128. [[CrossRef](#)]
45. Vesala, T.; Huotari, J.; Rannik, Ü.; Suni, T.; Smolander, S.; Sogachev, A.; Launiainen, S.; Ojala, A. Eddy covariance measurements of carbon exchange and latent and sensible heat fluxes over a boreal lake for a full open-water period. *J. Geophys. Res. Atmos.* **2006**, *111*. [[CrossRef](#)]
46. Vale, R.; Santana, R.; Gomes, A.C.; Tóta, J. Increased nocturnal CO<sub>2</sub> concentration during breeze circulation events in a tropical reservoir. *Ambient. Água Interdisc. J. Appl. Sci.* **2018**. [[CrossRef](#)]
47. Mulholland, P.J.; Fellows, C.S.; Tank, J.L.; Grimm, N.B.; Webster, J.R.; Hamilton, S.K.; Martí, E.; Ashkenas, L.; Bowden, W.B.; Dodds, W.K.; et al. Inter-biome comparison of factors controlling stream metabolism. *Freshw. Biol.* **2001**, *46*, 1503–1517. [[CrossRef](#)]
48. Bott, T.L.; Montgomery, D.S.; Newbold, J.D.; Arscott, D.B.; Dow, C.L.; Aufdenkampe, A.K.; Jackson, J.K.; Kaplan, L.A. Ecosystem metabolism in streams of the Catskill Mountains (Delaware and Hudson River watersheds) and Lower Hudson Valley. *J. N. Am. Benthol. Soc.* **2006**, *25*, 1018–1044. [[CrossRef](#)]
49. Naiman, R.J. The annual pattern and spatial distribution of aquatic oxygen metabolism in boreal forest watersheds. *Ecol. Monogr.* **1983**, *53*. [[CrossRef](#)]
50. Dawson, J.J.C.; Billett, M.F.; Hope, D. Diurnal variations in the carbon chemistry of two acidic peatland streams in north-east Scotland. *Freshw. Biol.* **2001**, *46*, 1309–1322. [[CrossRef](#)]
51. Jähne, B.; Münnich, K.O.; Bössinger, R.; Dutzi, A.; Huber, W.; Libner, P. On the parameters influencing air-water gas exchange. *J. Geophys. Res.* **1987**, *92*, 1937–1949. [[CrossRef](#)]
52. Schubert, M.; Forster, R.M. Sources of variability in the factors used for modelling primary productivity in eutrophic waters. *Hydrobiologia* **1997**, *349*, 75–85. [[CrossRef](#)]
53. Helbling, E.W.; Banaszak, A.T.; Villafane, V.E. Global change feed-back inhibits cyanobacterial photosynthesis. *Sci. Rep.* **2015**, *5*, 14514. [[CrossRef](#)]
54. Sand-Jensen, K.; Pedersen, M.F.; Laurentius, S. Photosynthetic use of inorganic carbon among primary and secondary water plants in streams. *Freshw. Biol.* **1992**, *27*, 283–293. [[CrossRef](#)]
55. Rich, S.M.; Pedersen, O.; Ludwig, M.; Colmer, T.D. Shoot atmospheric contact is of little importance to aeration of deeper portions of the wetland plant *Meionectes brownii*; submerged organs mainly acquire O<sub>2</sub> from the water column or produce it endogenously in underwater photosynthesis. *Plant Cell Environ.* **2013**, *36*, 213–223. [[CrossRef](#)]
56. Krause-Jensen, D.; Sand-Jensen, K. Light attenuation and photosynthesis of aquatic plant communities. *Limnol. Oceanogr.* **1998**, *43*, 396–407. [[CrossRef](#)]
57. Pedersen, O.; Colmer, T.D.; Sand-Jensen, K. Underwater photosynthesis of submerged plants—Recent advances and methods. *Front. Plant Sci.* **2013**, *4*, 140. [[CrossRef](#)] [[PubMed](#)]
58. Turner, R.E.; Rabalais, N.N.; Alexander, R.B.; McIsaac, G.; Howarth, R.W. Characterization of nutrient, organic carbon, and sediment loads and concentrations from the Mississippi River into the northern Gulf of Mexico. *Estuaries Coasts* **2007**, *30*, 773–790. [[CrossRef](#)]
59. Borges, A.V.; Abril, G.; Darchambeau, F.; Teodoru, C.R.; Deborde, J.; Vidal, L.O.; Lambert, T.; Bouillon, S. Divergent biophysical controls of aquatic CO<sub>2</sub> and CH<sub>4</sub> in the World's two largest rivers. *Sci. Rep.* **2015**, *5*, 15614. [[CrossRef](#)] [[PubMed](#)]
60. Borges, A.V.; Darchambeau, F.; Teodoru, C.R.; Marwick, T.R.; Tamooh, F.; Geeraert, N.; Omengo, F.O.; Guérin, F.; Lambert, T.; Morana, C.; et al. Globally significant greenhouse gas emissions from African inland waters. *Nat. Geosci.* **2015**, *8*, 637–642. [[CrossRef](#)]

61. Descy, J.P.; Darchambeau, F.; Lambert, T.; Stoyneva, M.P.; Bouillon, S.; Borges, A.V. Phytoplankton dynamics in the Congo River. *Freshw. Biol.* **2017**, *62*, 87–101. [[CrossRef](#)]
62. Townsend, S.A.; Webster, I.T.; Schult, J.H. Metabolism in a groundwater-fed river system in the Australian wet/dry tropics: Tight coupling of photosynthesis and respiration. *J. N. Am. Benthol. Soc.* **2011**, *30*, 603–620. [[CrossRef](#)]



© 2018 by the authors. Licensee MDPI, Basel, Switzerland. This article is an open access article distributed under the terms and conditions of the Creative Commons Attribution (CC BY) license (<http://creativecommons.org/licenses/by/4.0/>).